Interplay between mobile genetic elements drives a fusion-deletion life cycle of plasmids to fuel antimicrobial resistance

Thomas Ipoutcha[1,2,*], Yiqing Wang[3], Eduardo P C Rocha[3], José R Penadés[1,2,4,*]

[1]Department of Infectious Disease, Imperial College London, SW7 2AZ, London, UK

[2]Centre for Bacterial Resistance Biology, Imperial College London, SW7 2AZ, London, UK

[3]Microbial Evolutionary Genomics, CNRS UMR3525, Institut Pasteur, Université Paris Cité, 75724 Paris, France.

[4]Veterinary School, Universidad CEU Cardenal Herrera, Alfara del Patriarca, 46115, Spain

***Corresponding authors:** Thomas Ipoutcha (t.ipoutcha@imperial.ac.uk); José R Penadés (j.penades@imperial.ac.uk)

ORCID identifier: Thomas IPOUTCHA (0000-0001-6266-9381),
ORCID identifier: Yiqing WANG
ORCID identifier: Eduardo P C ROCHA (0000-0001-7704-822X)
ORCID identifier: José R PENADÈS (0000-0002-6439-5262)

Preprint servers: BioRxiv

Keywords: evolutiuon, AMR, diversity, adaptation, *Staphylococcus*

The authors declare no conflict of interest.

Summary

Plasmids are key drivers of bacterial adaptation, yet the mechanisms that generate their diversity remain poorly understood. Here, we show that mobile genetic elements (MGEs) orchestrate a fusion-deletion life cycle that drives the emergence of multireplicon, multidrug-resistant plasmids in *Staphylococcus aureus*. Large-scale genomic analyses reveal that multireplicon plasmids are widespread and strongly enriched in transposases. Using experimental assays, we demonstrate that rare MGE-mediated fusion events, via homologous recombination or transposition, combine distinct plasmids into single multireplicon elements, expanding gene content and transfer potential. Antibiotic pressure selectively enriches these fused plasmids, rescuing bacterial populations under stress, whereas opposing selective forces, including phage predation**,** favor deletion derivatives that preserve essential functions and transmissibility. This cyclical process generates dynamic plasmid repertoires with conserved backbones and diverse accessory modules. We propose that MGE-driven fusion-deletion cycles represent a general principle of plasmid evolution, explaining the rapid emergence and persistence of multidrug-resistant plasmids across bacterial pathogens.

Introduction

Plasmids are central drivers of bacterial evolution, mediating the horizontal transfer of genes that confer antibiotic resistance, virulence, and metabolic versatility (Smillie et al., 2010). Their mobility enables rapid adaptation across ecological and clinical contexts and has been a major force in the emergence and global spread of multidrug-resistant pathogens, particularly among the ESKAPE bacteria (Partridge et al., 2018). As antimicrobial resistance (AMR) continues to escalate worldwide (Savoldi et al., 2019; World-Health-Organization, 2022), understanding the evolutionary principles that govern plasmid diversity has become a critical priority.

Across bacteria, plasmids adopt distinct mobility strategies, ranging from large self-transmissible elements (conjugative) to smaller mobilizable or non-transmissible plasmids that rely on other mobile elements, for dissemination (Smillie et al., 2010). Conjugative plasmids carry all the machinery required for self-transfer between bacteria, mobilizable plasmids carry partial transfer functions and require a conjugative plasmid to move, and non-transmissible plasmids lack the capacity for autonomous transfer (Smillie et al., 2010). Conjugative plasmids are generally larger (>50 kb, > 25kb in firmicutes) (Ares-Arroyo et al., 2023), reflecting the size of their transfer machinery. In contrast, across all analyzed species, mobilizable and non-transmissible plasmids display a bimodal size distribution, with peaks corresponding approximately to the size of phage genomes (~40–45 kb) and phage-inducible chromosomal island (PICI) elements (~10–20 kb) (Fillol-Salom et al., 2018; Smillie et al., 2010). This bimodality explains how smaller plasmids can still be mobilized via phage- or PICI-mediated generalized transduction, despite lacking conjugation genes (Humphrey et al., 2021).

These strategies of transfer impose strong physical and ecological constraints on plasmid size, creating a fundamental trade-off between mobility and gene content. Smaller plasmids are transferred using different mechanisms but encode fewer accessory genes, whereas larger plasmids can carry extensive adaptive cargo but can only be transferred by conjugation. Despite these constraints, natural plasmid populations display remarkable diversity in size,

structure, and gene content, raising a central unresolved question: how is plasmid diversity generated and maintained in the face of strong selective and physical limitations?

Although plasmids can gain, lose, and rearrange genetic material, the evolutionary dynamics governing these processes remain poorly understood. Several recent studies have shown that plasmid fusion can generate multireplicon plasmids by combining genetic material from distinct elements (Cazares et al., 2025; Douarre et al., 2020; H. Liu et al., 2024; Z. Liu et al., 2025; Rozwandowicz et al., 2018; Wang et al., 2022). However, these observations do not address how frequent such fusion events are in natural populations, how they are integrated into long-term evolutionary dynamics, or how plasmids simultaneously maintain conserved functional backbones, constrained size distributions, and extensive accessory gene diversity.

Here, we propose that, as observed for other mobile genetic elements, plasmids also follow a defined life cycle that enables their persistence and propagation in nature. In this life cycle, rare fusion events transiently expand genetic content through plasmid co-integration, whereas opposing selective forces eliminate excess DNA, preserving essential functions and transmissibility. Our results provide a mechanistic explanation for how plasmids generate extensive genetic diversity while maintaining conserved backbones and constrained size distributions, reconciling plasmid adaptability with long-term evolutionary stability.

Results

Plasmid diversity and fusion signatures in *S. aureus*

To determine how plasmid diversity is generated and maintained despite strong constraints on size and mobility, we analyzed plasmids from *Staphylococcus aureus*, a species in which plasmid-mediated gene transfer is central to adaptation, virulence, and antimicrobial resistance. The coexistence of conjugative, mobilizable, and non-transmissible plasmids within the same populations provides a natural system to assess how different mobility strategies, genetic architectures, and fusion signatures are distributed at scale.

96 We compiled a dataset of 2,564 complete *Staphylococcus* plasmids from the PLSDB
97 database, including 1,649 from *S. aureus*. Plasmids were classified according to predicted
98 mobility and replicon content (Fig. 1). Among plasmids carrying at least one identifiable Rep
99 gene (2,308/2,564), 7% were conjugative (159), 22% mobilizable (516), 43% encoded an
100 origin of transfer (997), and 31% were non-transmissible (636) (Fig. 1A).

101 Unexpectedly, nearly half of all plasmids (49%, 1,255/2,564) carried more than one Rep
102 gene, indicative of plasmid fusion events and the formation of multireplicon plasmids (Fig. 1B).
103 Fusion signatures were particularly enriched among plasmids that rely on conjugation for
104 transfer, whereas they were substantially less frequent among non-transmissible plasmids
105 (Fig. 1B). Consistent with plasmid co-integration, multireplicon plasmids were significantly
106 larger than single-replicon plasmids (Fig. 1C), indicating that fusion contributes directly to
107 plasmid expansion.

108 Analysis of replicon families revealed that fusion signatures were not confined to a small
109 subset of plasmids but were distributed across most lineages (Fig. 1D; Fig. S1A). Small
110 plasmid families, such as those carrying the RepL replicon, were typically restricted to sizes of
111 2–8 kb unless incorporated into larger fused plasmids (Table S1). In contrast, RepA_N and
112 Inc18 families showed particularly high frequencies of fusion, suggesting that certain replicon
113 types play a central role in plasmid co-integration and diversification. Together, these results
114 demonstrate that plasmid fusion is not a rare or exceptional event in *S. aureus*, but a
115 widespread feature of plasmid populations, providing a potential mechanism for generating
116 genetic diversity despite strong constraints on plasmid size and mobility.

117 **Association of mobile genetic elements with plasmid fusion**

118 Plasmid fusion requires the presence of identical or highly similar sequences in distinct
119 plasmids. Because insertion sequences (IS) are involved in plasmid evolution and are
120 overrepresented in plasmids of clinical importance (Sastre-Dominguez et al., 2024; Varani et
121 al., 2021), transposases are strong candidates for mediating such co-integration events.
122 Indeed, several cases have shown that IS elements, particularly those of the IS6 family (e.g.,

123 IS257), can generate transient plasmid co-integrates in *Escherichia coli* (Goswami et al., 2020;
124 Harmer et al., 2014; He et al., 2015b; Osborn et al., 2000; Snaith et al., 2023) and
125 *Staphylococcus aureus* (Leelaporn et al., 1996; Morton et al., 1995; Yui Eto et al., 2019). To
126 determine whether IS-mediated fusion is a widespread feature of plasmid populations, we
127 analyzed the *Staphylococcus* plasmid dataset for the presence of insertion sequences.

128 BLASTn analysis revealed that 40% of *Staphylococcus* plasmids carry IS257, with a
129 striking enrichment among multireplicon plasmids (58% in plasmids with two replicons and up
130 to 98% in plasmids with four replicons, compared with 22% in single-replicon plasmids) (Fig.
131 S2B). Conjugative and *oriT*-encoding plasmids, both of which display elevated fusion
132 frequencies, were also enriched for IS257 (52% and 50%, respectively) (Fig. S2C). In contrast,
133 RepL plasmids showed low frequencies of both IS257 carriage (12%) and fusion signatures
134 (10%) (Fig. S1A, S2A). Conversely, replicon families with high fusion prevalence, such as
135 RepA_N, were strongly enriched for IS6-family elements (67%).

136 ISBli29, which encodes a Mu-family transposase, was the second most abundant insertion
137 sequence in *Staphylococcus* plasmids and showed a similar association with plasmid fusion.
138 ISBli29 was rare in single-replicon plasmids (3%) but enriched in multireplicon plasmids (18–
139 26%) (Fig. S2B). Notably, ISBli29 was particularly prevalent in Rep3 plasmids (39%), a family
140 in which IS6 elements are less common (27%) yet fusion frequencies are high (77%) (Fig.
141 S2A). Both IS6 and ISBli29 were associated with increased plasmid size (Fig. S2D), consistent
142 with their role in promoting plasmid co-integration (Choi & Harshey, 2010; Varani et al., 2021).

143 Together, these results identify transposable elements as central and pervasive drivers of
144 plasmid fusion, providing a mechanistic link between the widespread occurrence of
145 multireplicon plasmids and the enrichment of insertion sequences in plasmid genomes.

146 **Plasmid families with conserved backbones show evidence of modular evolution**

147 To investigate how plasmids diversify while maintaining conserved core functions, we asked
148 whether plasmids sharing the same replicon type (that is, the same replication machinery),

149 also vary in size and gene content. If so, this would indicate that plasmids undergo repeated
150 gain and loss of accessory modules over time. We focused on plasmids carrying the RepA_N
151 replicon, which display a high prevalence of multireplicon architectures (Fig. S1A). Within this
152 group, we analyzed two representative subfamilies, Rep15 and Rep20 (Fig. 2A), both of which
153 frequently carry IS257 (Fig. 2B) and exhibit substantial size variability (Fig. 2C).

154 Comparative sequence analyses revealed highly conserved backbone regions within each
155 subfamily, contrasted by extensive variation in accessory content (Fig. 2D,E). Many accessory
156 modules corresponded to complete or partial plasmid sequences flanked by IS257 elements,
157 often containing additional insertion sequences, suggesting a role for transposases in both the
158 acquisition and rearrangement of these modules. In the Rep15 subfamily, 90% of plasmids
159 retained a conjugation module, whereas a minority lacked this region, consistent with deletion
160 events (Table S1; Fig. 2D). Conversely, Rep20 plasmids were predominantly *oriT*-encoding or
161 mobilizable, but a small subset carried conjugation machinery, consistent with sporadic
162 acquisition events (Table S1; Fig. 2E).

163 Despite frequent fusion and rearrangement, plasmid sizes in both Rep15 and Rep20
164 remained tightly constrained, with very few exceeding 45 kb (Fig. 2C). This pattern extended
165 to the full *Staphylococcus* plasmid dataset, where only 6% of plasmids (162/2,564) were larger
166 than 45 kb (Table S1). Notably, this size threshold corresponds to the packaging capacity of
167 most *Staphylococcus* transducing phages (Deghorain & Van Melderen, 2012), supporting the
168 idea that phage-mediated transfer imposes an upper limit on plasmid size (Humphrey et al.,
169 2021).

170 Together, these observations indicate that plasmids with conserved replication backbones
171 are not static entities but undergo continuous, modular remodeling through the gain and loss
172 of accessory regions. This process generates extensive diversity in antimicrobial resistance
173 gene combinations while preserving core plasmid functions. The mechanisms underlying this
174 modular evolution are explored in the following sections.

175 **Experimental evidence for plasmid fusion**

176 To directly test the mechanisms driving plasmid fusion, we selected naturally occurring
177 plasmids that carry at least one IS257 element and belong to replicon families showing strong
178 bioinformatic signatures of fusion (Fig. S1A–S2A). pGO1 is a conjugative plasmid from the
179 Rep15 family (Caryl & O'Neill, 2009) for which smaller conjugative and non-conjugative
180 derivatives have been described (Humphrey et al., 2021) (Fig. S3A). pWBG731 is a
181 conjugative plasmid carrying two functional replication genes, Rep15 and Rep20, along with a
182 smaller non-conjugative derivative retaining only Rep20 (Yui Eto et al., 2019). As a
183 representative small, non-transmissible plasmid, we used pUR3912, which belongs to the
184 Rep27 family (Gómez-Sanz et al., 2013).

185 To determine whether plasmid fusion can occur at the population level, we introduced
186 pairs of large conjugative and small non-transmissible plasmids into the same *S. aureus* strain
187 (pGO1 or pWBG731 together with pUR3912), allowed cultures to propagate, and extracted
188 plasmid DNA. We designed PCR primers to specifically detect fusion junctions generated by
189 homologous recombination between IS257 elements (Fig. S3A). Using this approach, we
190 amplified the expected fusion products and confirmed their junction sequences by Sanger
191 sequencing (Fig. S3B).

192 These results demonstrate that plasmid fusion can occur naturally through homologous
193 recombination at IS257 sites. However, while PCR detection establishes the occurrence of
194 fusion events, it does not inform on their frequency within the population or the selective forces
195 that promote their persistence, questions that we address in the following experiments.

196 **Antibiotic selection enriches fused plasmids**

197 Plasmid fusion can occur naturally, but such events are intrinsically rare, in part because
198 homologous recombination rate is low in *S. aureus* (Vos & Didelot, 2009). This rarity contrasts
199 sharply with the high prevalence of multireplicon plasmids observed in genomic databases,
200 suggesting that fused plasmids must be strongly selected in nature to reach detectable
201 frequencies.

202 We hypothesized that strong antibiotic pressure could provide such selection, by favoring
203 fusion between a conjugative plasmid and a non-transmissible plasmid and thereby rescuing
204 bacterial populations under conditions that neither plasmid alone could withstand. To test this,
205 we designed an experimental system in which a donor strain carrying both a large conjugative
206 plasmid (pGO1, pGO1-EvoF, or pWBG731) and a smaller non-transmissible plasmid (pGO1-
207 Evocat, pTI144, or pUR3912) was co-cultured with a recipient strain bearing a distinct antibiotic
208 resistance marker. Under these conditions, survival under three-antibiotic selection could only
209 occur through plasmid fusion followed by conjugative transfer (Fig. 3A).

210 Cultures were plated under two selection regimes: two antibiotics, to measure baseline
211 conjugation efficiency, and three antibiotics, to specifically select for fused plasmids. Under
212 two-antibiotic conditions, conjugation efficiencies were high, yielding 10^4-10^6 transconjugants
213 per mL for pGO1 and pWBG731 (Fig. 3B, S3C). In contrast, only a small number of colonies
214 were recovered under three-antibiotic selection. To determine whether these colonies carried
215 fused plasmids, three isolates from each condition were used as donors in secondary
216 conjugation assays into a fresh recipient strain. In all cases, conjugation efficiencies returned
217 to levels comparable to those of the parental conjugative plasmids (10^3-10^6 transconjugants
218 per mL; Fig. 3C).

219 Long-read sequencing of these isolates confirmed that they carried fused plasmids
220 containing both the conjugative and non-transmissible elements (Fig. 3D, S3D). Because
221 fusion events occur prior to antibiotic selection (Fig. S3B), the reduction in transfer efficiency
222 between two- and three-antibiotic conditions provides an estimate of fusion frequency in the
223 population. Across all tested combinations, fusion events were 3-4 orders of magnitude less
224 frequent than standard conjugation, confirming that plasmid fusion is rare under baseline
225 conditions (Fig. 3B). Short-read sequencing of plasmids before and after fusion showed that
226 Rep27, which allows a high copy number, is ultimately detected at a level similar to that of the
227 large conjugative plasmid after fusion (Table S6).

228 Together, these results demonstrate that although plasmid fusion occurs infrequently,
229 strong antibiotic pressure can selectively enrich fused plasmids. By conferring conjugative
230 mobility to previously non-transmissible elements, fusion enables population survival under
231 multidrug stress and provides a selective route by which rare fusion events can rise to
232 prominence. This selective enrichment offers a mechanistic explanation for the widespread
233 prevalence of multireplicon plasmids observed in genomic databases.

234 **Homologous recombination and transposition shape plasmid fusion**

235 Plasmid fusion can arise through multiple molecular mechanisms, including homologous
236 recombination (HR) and transposition, both of which can contribute to plasmid diversification.
237 To define the role of IS257 in mediating fusion, we analyzed long-read sequencing data from
238 fused plasmids isolated during the antibiotic selection experiments (Fig. 3D; Fig. S3). In all
239 sequenced clones, IS257 elements flanked the fusion junctions, indicating that fusion occurred
240 either through HR between IS257 copies or via IS257-mediated transposition.

241 To distinguish between these mechanisms, we examined fusion junctions for signatures
242 of transposition, specifically the presence of 7-bp direct repeats characteristic of IS6-family
243 transposase activity (Varani et al., 2021). In two clones (TI226 and TI228), fusion junctions
244 were flanked by newly generated IS257 copies and 7-bp direct repeats (Fig. 3D; Fig. S3D),
245 consistent with transposition events. These insertions occurred at multiple sites within the
246 small non-transmissible plasmid pUR3912 and were independent of its native IS257 element
247 (Fig. S4C). In contrast, four clones (TI564, TI243, TI246, and TI249) lacked direct repeats, and
248 fusion occurred directly between pre-existing IS257 elements on each plasmid, consistent with
249 HR-mediated co-integration (Fig. S3D).

250 To experimentally test whether both HR and transposition can independently mediate
251 plasmid fusion, we constructed derivatives of pUR3912 lacking IS257 (pUR3912-noIS), as well
252 as a variant containing an alternative region of homology (the trimethoprim resistance gene)
253 shared with pGO1 and pWBG731 (Fig. S4A). Under selective conditions favoring fusion, all
254 plasmid variants supported population rescue following conjugation with pWBG731 and pGO1-

255 EvoF (Fig. S4B). Long-read sequencing confirmed plasmid fusion in all cases and revealed
256 junction architectures consistent with either HR or transposition (Fig. S4C–S4F). Analysis of
257 transposition-derived junctions identified a conserved 7-bp direct repeat motif, allowing
258 definition of a consensus insertion site (TTTWTAD) (Fig. S4C–S4D).

259 Together, these results demonstrate that plasmid fusion can be mediated by both
260 homologous recombination and transposition. Moreover, short regions of sequence homology,
261 including conserved replication genes, resistance determinants, or transposase sequences,
262 are sufficient to promote co-integration. This mechanistic flexibility provides a basis for the
263 widespread generation of plasmid diversity and illustrates how mobile genetic elements
264 facilitate rapid adaptation under selective pressures such as antibiotic exposure.

265 **Plasmid size does not impose a fitness cost after fusion**

266 Although plasmid fusion is frequent and widely represented in genomic databases, very few
267 *Staphylococcus* plasmids exceed 45 kb, even among those with clear fusion signatures (Fig.
268 1B). We considered three non-mutually exclusive explanations for this pattern: (i) a fitness cost
269 associated with carrying large plasmids, (ii) resolution of fused plasmids after co-integration,
270 and (iii) selection for deletions, potentially driven by phage-mediated transfer constraints.

271 To test whether increased plasmid size or the presence of multiple replication systems
272 imposes a fitness cost, we compared the growth of bacteria carrying fused plasmids with that
273 of strains carrying their unfused parental plasmids. Using fused plasmids generated in our
274 experimental system, we first assessed whether plasmid size correlated with reduced growth
275 (Fig. 4A). No consistent size-dependent fitness cost was detected. For example, the 76-kb
276 fused plasmid derived from pGO1 grew comparably to its parental plasmids pGO1 (54 kb) and
277 pGO1-EvoF (42 kb). The smallest derivative, pGO1-Evocat, displayed slightly faster growth,
278 likely reflecting the absence of conjugation machinery. Similarly, in the pWBG731 background,
279 fused plasmids of 78 kb and 102 kb grew as well as, or slightly better than, the smaller
280 pWBG731-TI144 (26 kb) and the original pWBG731 plasmid.

281 We next examined whether carrying two active replication systems within a single plasmid
282 affected bacterial fitness. We compared growth of strains harboring fused plasmids in which
283 one Rep gene was naturally inactivated during fusion with those retaining two functional Rep
284 genes (Fig. 4B). Again, no significant differences in growth were observed.

285 Together, these results indicate that neither increased plasmid size nor the presence of
286 multiple active replication systems imposes a detectable fitness cost under the conditions
287 tested. The predominance of smaller plasmids in natural populations therefore cannot be
288 explained by fitness limitations alone, implicating alternative selective forces, such as deletion
289 processes or phage-mediated constraints, in maintaining compact plasmid sizes.

290 **Resolution and deletion diversify fused plasmids**

291 Previous studies have shown that plasmids generated by transposition can sometimes resolve
292 back into their original components (Berg et al., 1998; Novick et al., 1986). To determine the
293 intrinsic fates of fused plasmids after co-integration, we examined the outcomes of fusion
294 events independently of their long-term selective success.

295 Using fused derivatives of pGO1–pUR3912 and pWBG731–pUR3912 generated in earlier
296 experiments, we exploited phage-mediated transduction while selecting for resistance
297 encoded by the smaller plasmid. Because large fused plasmids exceed the DNA packaging
298 capacity of most staphylococcal phages, colonies recovered under these conditions were
299 expected to reveal post-fusion processing events, including resolution or deletion (Fig. 4C).

300 Analysis of recovered colonies revealed two distinct mechanistic outcomes. In two
301 sequenced clones (TI267, TI273), the original small plasmid was regenerated, indicating
302 resolution of the co-integrated plasmid back into its parental components. In parallel, a second
303 class of colonies retained resistance markers associated with the large conjugative plasmid.
304 Among 35 colonies examined for pGO1–pUR3912 and 9 for pWBG731–pUR3912, 6 and 9
305 colonies, respectively, displayed this phenotype (Fig. 4C).

306 Long-read sequencing showed that these latter isolates carried novel intermediate-sized
307 plasmids generated by deletion rather than simple resolution (Fig. 4D). In one case, deletion
308 of the pGO1 backbone resulted in a pUR3912 derivative that acquired full conjugation
309 machinery, effectively converting it into a conjugative plasmid. In all sequenced cases, deletion
310 junctions were consistent with homologous recombination between IS257 elements (Fig. 4D).

311 Deletion events were also detected in the absence of phage infection. Using plasmids
312 carrying multiple IS257 copies, we amplified and sequenced recombination scars consistent
313 with IS257-mediated deletions occurring naturally at the population level (Fig. S5).

314 Together, these results demonstrate that fused plasmids act as diversification
315 intermediates**,** from which multiple evolutionary outcomes can arise, including resolution back
316 to parental plasmids and deletion-driven formation of novel chimeric elements.

317 **Phage pressure selectively enriches small plasmid derivatives**

318 While fused plasmids generate multiple derivative forms, the relative abundance of these
319 outcomes in natural populations is expected to depend on ecological selection. In particular,
320 bacteriophages impose strong physical constraints on DNA packaging, potentially favoring
321 smaller plasmid variants capable of being transduced.

322 To test whether phage pressure selectively enriches specific post-fusion outcomes,
323 strains carrying multireplicon plasmids larger than 45 kb were infected with phages 80α or
324 ϕ2339 and subjected to transduction into recipient strains under defined selection regimes. We
325 predicted that phage-mediated transfer would act as a filter, enriching for plasmid variants
326 compatible with phage packaging.

327 Consistent with this prediction, transduction recovered a diverse spectrum of plasmid
328 derivatives in all plasmid–phage combinations tested (Fig. 5A-B). Long-read sequencing
329 revealed plasmids of intermediate sizes (33.5-44.5 kb) with distinct architectures, including
330 deletion derivatives, resolved parental plasmids, and novel combinations of resistance genes
331 and conjugation modules (Fig. 5; Fig. S6).

332 Importantly, growth assays showed no detectable fitness cost associated with these
333 smaller derivatives relative to their fused precursors (Fig. S6), indicating that their enrichment
334 was driven by transfer efficiency rather than growth advantage.

335 Together, these results demonstrate that bacteriophage pressure does not generate
336 plasmid diversity de novo, but selectively amplifies specific outcomes produced by plasmid
337 fusion, favoring smaller, transducible variants. This selective filtering explains how plasmid
338 size remains constrained in nature while preserving extensive genetic diversity.

339 **A fusion-diversification-selection life cycle of plasmids**

340 Integrating our bioinformatic, genetic, and experimental data, we identify a plasmid life cycle
341 characterized by alternating phases of fusion, diversification, and selection (Fig. 6). Under
342 antibiotic pressure, rare fusion events arise through multiple molecular mechanisms, including
343 transposition, homologous recombination between insertion sequences, or recombination at
344 other shared regions such as resistance cassettes or replication genes. These events generate
345 multireplicon plasmids that combine genetic material from distinct elements and mobilize
346 previously non-transmissible plasmids, rescuing bacterial populations under stress.

347 Following co-integration, fused plasmids act as transient diversification intermediates.
348 They can resolve back into their parental components or undergo deletion to form
349 intermediate-sized chimeric plasmids that retain key functional modules. Phage-mediated
350 transduction then selectively enriches smaller, transducible derivatives, imposing a strong
351 constraint on plasmid size while preserving genetic diversity.

352 Together, these results define a fusion-diversification-selection cycle that explains how
353 plasmid populations maintain conserved backbones, constrained size distributions, and
354 extensive accessory gene diversity.

355 **Discussion**

356 Plasmids are central engines of bacterial adaptation, yet the evolutionary forces shaping their
357 diversity remain poorly understood. Here, we describe a plasmid life cycle in *S. aureus*

358 governed by alternating phases of fusion, diversification, and selection. Rare fusion events,
359 mediated by homologous recombination, transposition, or short regions of shared homology,
360 generate multireplicon plasmids that expand genetic repertoires and mobilization potential. By
361 transiently linking otherwise independent elements, fusion enables the mobilization of
362 previously non-transmissible plasmids and can rescue bacterial populations under strong
363 antibiotic pressure.

364 Our results show that fused plasmids are not stable evolutionary endpoints but transient
365 diversification intermediates. Following co-integration, plasmids may resolve into their original
366 components or undergo deletion to generate intermediate-sized chimeric plasmids retaining
367 key functional modules. These branching trajectories substantially increase genetic variability
368 within recipient populations, producing a spectrum of plasmid architectures from a single fusion
369 event and helping to explain how extensive plasmid diversity can arise despite the intrinsic
370 rarity of fusion.

371 Ecological selection then acts on this diversity. In *S. aureus*, bacteriophage predation
372 imposes a strong physical constraint on plasmid size, selectively enriching variants compatible
373 with phage-mediated transduction. Deletion derivatives and resolved plasmids that fall below
374 phage packaging limits are preferentially transmitted, whereas very large fused plasmids are
375 disfavored. Importantly, this size-dependent trade-off is not imposed by phages alone:
376 staphylococcal pathogenicity islands (SaPIs) further restrict plasmid mobility by packaging only
377 small DNA molecules, typically below ~15 kb, thereby favoring even more compact plasmid
378 architectures. Because smaller derivatives often retain conjugation or mobilization functions
379 and incur little or no fitness cost, they can persist and spread efficiently. Together, antibiotic-
380 driven fusion and phage- and SaPI-mediated size constraints create a fusion–diversification–
381 selection cycle that explains conserved plasmid backbones, constrained size distributions, and
382 extensive accessory gene diversity.

383 IS emerges as central catalysts of this process. It facilitates both fusion and deletion
384 through homologous recombination and transposition, enabling rapid structural

385 rearrangements across short regions of homology. This role is consistent with observations in
386 other bacterial species, where IS6-family elements mediate plasmid co-integration via similar
387 mechanisms (Goswami et al., 2020; Harmer et al., 2014; He et al., 2015a). Importantly, IS-
388 mediated rearrangements can generate stable plasmid variants that persist under selection
389 rather than remaining purely transient. Conjugative plasmids, display particularly high fusion
390 frequencies, mirroring patterns reported in *Escherichia coli* and other species where IS density
391 is elevated near antimicrobial resistance genes (Che et al., 2021; Pfeifer & Rocha, 2024;
392 Sastre-Dominguez et al., 2024).

393 Beyond IS elements, other conserved genetic features, including resistance cassettes and
394 replication genes, can also serve as substrates for homologous recombination. While
395 replication genes represent potential recombination targets, plasmid incompatibility limits the
396 stable coexistence of identical replicons within the same cell (Novick, 1987), potentially
397 constraining diversification among closely related plasmids. How these opposing forces
398 interact to shape long-term plasmid evolution remains an important open question.

399 Our findings help explain how rare genetic events can have disproportionate population-
400 level consequences. Although fusion and deletion occur infrequently, strong selective
401 pressures - antibiotics favoring fusion-derived mobilization and phages and SaPIs favoring
402 compact, transducible plasmids - amplify their evolutionary impact. This dynamic explains why
403 multireplicon plasmids and fusion signatures are widespread in genomic databases despite
404 low baseline frequencies and aligns with recent work showing that restricted plasmid mobility
405 can promote population-level diversity under combined antibiotic and phage pressure.

406 Importantly, this life-cycle framework also aligns with the historical trajectory of plasmid
407 evolution (Cazares et al., 2025). Pre-antibiotic-era of *Enterobacteriaceae* plasmids were
408 largely devoid of resistance genes and rarely fused, whereas post-antibiotic-era plasmids have
409 evolved into multireplicon, self-transmissible elements that dominate contemporary
410 populations. While previous studies documented plasmid remodeling (Cazares et al., 2025; Z.
411 Liu et al., 2025), the underlying molecular mechanisms remained unclear. Our results provide

412 mechanistic insight into this transition: antibiotics select for rare fusion events that combine
413 multiple resistance determinants, while phage and SaPI pressure (Humphrey et al., 2021)
414 constrain plasmid size, shaping the mosaic architecture of modern resistance plasmids. By
415 linking rare fusion and deletion events to strong ecological selection, we propose a stabilizing
416 framework explaining how quickly, dramatic plasmid remodeling can repeatedly arise, persist,
417 and spread in natural populations, accounting for the rapid emergence and global
418 dissemination of multidrug-resistant plasmids.

419 An important layer not explicitly incorporated into our model is the role of plasmid-encoded
420 phage defense systems. Defense mechanisms such as restriction–modification systems or
421 abortive infection modules may influence which plasmid variants persist following fusion or
422 deletion. Plasmids combining antimicrobial resistance with effective phage defense could be
423 preferentially retained, potentially reshaping both gene content and size constraints.
424 Incorporating phage defense into future models will refine our understanding of how plasmid
425 mobility, gene content, and architecture are jointly optimized under complex ecological
426 pressures.

427 Although this study focuses on *S. aureus*, the underlying principles are likely
428 generalizable. Multireplicon plasmids, IS-mediated fusion, and deletion events are reported in
429 *Enterobacteriaceae*, *Klebsiella*, and *E. (Douarre et al., 2020; Giordano et al., 2018; He et al.,*
430 *2015a)*, suggesting that plasmid life cycles represent a broadly conserved evolutionary
431 strategy for balancing genetic innovation with mobility. However, the strength of size
432 constraints likely varies across taxa, reflecting differences in phage and SaPI ecology and
433 highlighting mobile genetic elements as critical, yet underappreciated, drivers of plasmid
434 evolution.

435 By integrating mechanistic insight with ecological selection, this study provides a unifying
436 framework for understanding plasmid diversification, the emergence of multidrug resistance,
437 and the long-term evolutionary impact of antibiotic use. It also suggests potential intervention

438 strategies, such as exploiting phage- or SaPI-mediated size constraints or targeting plasmid
439 recombination pathways, to disrupt the propagation of resistance determinants.
440

441 **Materials and Methods**

442 **Oligonucleotides and plasmids.** All oligonucleotides used in this study were supplied by
443 Sigma and are listed in Table S5-A. All plasmids constructed and used in this study are listed
444 in Table S5-B.

445 **Bacterial strains and growth conditions.** The bacterial strains used in this study are listed
446 in Table S5-C. For all experiments, *S. aureus* was grown in Tryptic Soy Broth (TSB) at 37 °C
447 with shaking (180 rpm) overnight until stationary phase. For enumeration of colony-forming
448 units (CFU) on solid media, cultures were plated on Tryptic Soy Agar (TSA) and incubated at
449 37 °C. When required, the media was supplemented with the following antibiotic
450 concentrations: gentamicin 10 µg/ml; erythromycin 10 µg/ml; trimethoprim 20 µg/ml;
451 chloramphenicol 10 µg/ml; $CdCl_2$ 100 µM; tetracycline 3 µg/ml; rifampicin 10 µg/ml.
452 When using *Saccharomyces cerevisiae (*provided by Dr. Carole Lartigue, INRAE) as a cloning
453 platform, *S. cerevisiae* VL6-48N was grown in YPDA broth (Takara, 630464) overnight at 30
454 °C with shaking (200 rpm). When required, minimal SD medium (SD-Trp broth; Takara, 630411
455 and 630413) was used at 30 °C with shaking at 220 rpm.

456 **Bioinformatic analyses.**
457 3,076 *Staphylococcus* plasmids were downloaded from PlasmidScope database (version
458 2024-12-04, all the plasmids were collected from PLSDB). After removing potential
459 chromosomal contigs and merging identical sequences, 2,564 non-redundant complete
460 plasmids in a size range of 2-170 kb were kept for the further analysis (Supplementary Table
461 S1).

462 Plasmid mobility typing was performed using MacSyFinder v2.1.4 with CONJScan model
463 v2.0.1. OriT sequences were searched using BLASTn (with parameter -task blastn-short,
464 identity > 80% and coverage > 80%) with 117 experimentally valid oriT sequences from OriTDB
465 v2.0, the best hit from overlapping hits was kept. Plasmid mobility type are classfied into
466 plasmid encoding oriT sequence (pOriT), plasmid encoding relaxase (pMOB), conjugative
467 plasmid (pCONJ), decayed conjugative plasmid (pdCONJ), and plasmid lacking mobility
468 (pNT). 23 plasmids with mobility type “pdCONJ” are grouped into “pMOB” in the further
469 analysis.

470 Plasmid replicon typing was performed using PlasmidFinder v2.1.1 and replicon database
471 v2.2.0 (with parameters -t 0.8 -l 0.6, identity > 80% and coverage > 60%), the best hit from
472 overlapping hits was kept (Supplementary Table S2).

473 Replicon co-occurrence networks were plotted using Cytoscape v3.10.3.

474 Insertion sequence IS*6* and IS*Bli29* were detected using digIS v1.2 (Supplementary Table S3)
475 and IS*6* transposase sequences were cross valided using Blastn with a pre-build blast
476 database of Tncentral and ISFinder (version 2025-05-16), for each query the best hit was kept
477 (Supplementary Table S4).

478 **Detection deletion and fusion event in *Staphylococcus*.** Bacterial strain *S. aureus* RN4220
479 containing one or combinations of plasmids was cultured overnight, and plasmids were
480 extracted from 1 mL of culture using the ZR BAC DNA Miniprep Kit (Zymo Research, D4049).
481 PCRs were performed using Advantage II HF polymerase (Takara), following the
482 manufacturer's recommendations.

483 **Big plasmid construction.** The natural plasmid pGO1 lacking the conjugative machinery and
484 containing a chloramphenicol resistance gene was constructed in the non-commercial
485 *Saccharomyces cerevisiae* VL6-48N strain, as previously described (Kouprina & Larionov,
486 2008; Lee et al., 2015) and (Ruiz et al., 2019) with several modifications. Overlapping PCR
487 products and YAC (200 ng of each PCR product and 100 ng of linearized YAC in 10 µL water)
488 were co-transformed into VL6-48N. Individual yeast colonies were picked and streaked onto
489 SD-Trp plates, incubated for 2 days at 30°C, and then patched onto fresh SD-Trp plates and
490 incubated for another 2 days at 30°C. Total genomic DNA was extracted from yeast
491 transformants according (Kouprina & Larionov, 2008). PCRs were performed using
492 Advantage II HF polymerase (Takara), following the manufacturer's recommendations.

493 **Small plasmid construction.** Small pUR3912 derivatives lacking IS256, or in which IS256
494 was replaced by a sequence allowing homologous recombination with pGO1 and pWBG731,
495 and carrying the trimethoprim resistance gene, were constructed in *S. aureus* RN4220.
496 Overlapping PCR fragments were generated and assembled using the HiFi DNA Assembly Kit
497 (NEB). The reaction products were dialyzed on a membrane filter for 5 min, and the remaining
498 mixture was transformed into *S. aureus* RN4220 (2,200 kV, 100 Ω, 2 mm) and plated on TSA
499 containing erythromycin. Colonies were then analyzed, and plasmids were sequenced.

500 **Bacterial growth curves.** Growth kinetics were assessed using *Staphylococcus aureus*
501 RN4220 derivatives carrying the indicated plasmids. Overnight cultures were inoculated into
502 fresh Tryptic Soy Broth (TSB) at a 1:100 dilution and grown at 37 °C with shaking (180 rpm).
503 Cultures were transferred to 96-well flat-bottom plates (200 µL per well; three technical
504 replicates per strain), and optical density at 600 nm (OD600) was measured every 10 min for
505 24 h using a microplate reader with continuous orbital shaking between reads.

506 **Phage infection.** Bacterial cultures containing the appropriate plasmid were grown to an
507 OD600 of 0.15. One milliliter of culture was mixed with 100 µL of phages supplemented with 5
508 mM $CaCl_2$ and incubated at 30°C for 3 h, followed by overnight incubation at room
509 temperature. The resulting phage lysate was filtered to remove remaining bacterial cells.

510 **Phage titer.** *S. aureus* RN4220 was grown overnight, then subcultured at a 1:50 dilution into
511 fresh TSB and grown to an OD600 of 0.2. Bacterial lawns were prepared by mixing 100 µL of
512 cells with phage top agar (PTA, supplemented with $CaCl_2$ to a final concentration of 5 mM) and
513 pouring the mixture onto PBA plates supplemented with 5 mM $CaCl_2$. Serial dilutions of phage
514 lysates were prepared in phage buffer (50 mM Tris, pH 8; 1 mM $MgSO_4$; 4 mM $CaCl_2$; 100 mM
515 NaCl) and spotted onto the bacterial lawns, which were then incubated overnight at 37°C.
516 Plaques were counted and used to quantify the phage produced during infection.

517 **Plasmid transduction.** *S. aureus* RN4220 was grown in TSB to an OD600 of 1.4. For
518 transduction experiments, 100 µL of phage lysates were added to each culture along with 5
519 mM $CaCl_2$. The cultures were incubated statically at 37°C for 30 min and then plated onto TSA
520 plates containing 17 mM sodium citrate and the appropriate antibiotic for selection of the
521 expected plasmid. Plates were incubated for 24–48 h, and colonies were counted. The transfer
522 efficiency (TE) per donor cell was calculated as the number of Transductant Units (TrU) per
523 mL divided by the number of donor colony-forming units (CFU) per mL (6.5×10^7 CFU/mL for
524 a culture with an OD600 of 0.15).

525 **Statistical analyses.** Plasmid encoding multiple- / single- replicon was modeled using a
526 binomial generalized linear model using glm (R package stats v4.4.3, with parameter family =
527 binomial(link='logit')). The effect of plasmid size (log10 transformed), IS_presence (plasmid
528 encoding transposase of IS*6*/ IS*Bli29* or not), and plasmid mobility types are tested**.**

529

530 Supporting information

531
532 Table S1-S6
533

534 Acknowledgements and funding sources

535 This work was supported by grants MR/X020223/1, MR/M003876/1, MR/V000772/1
536 and MR/S00940X/1 from the Medical Research Council (UK), BB/V002376/1 and
537 BB/V009583/1 from the Biotechnology and Biological Sciences Research Council

(BBSRC, UK), and EP/X026671/1 from the Engineering and Physical Sciences Research Council (EPSRC, UK) to J.R.P. Thank you to Dr Carole Lartigue from INRAE for providing the VL6-48N strain, to Dr Joshua Ramsay from Curtin University for providing pWBG731 strain and to Daniel Sin for help with plotting.

Author contributions

J.R.P. and T.I. conceived the study; T.I and Y.W. conducted the experiments; T.I., Y.W., E.R., and J.R.P. analyzed the data; J.R.P. and T.I. wrote the manuscript.

Declaration of interests

The authors declare no competing interests.

References

Ares-Arroyo, M., Coluzzi, C., & Rocha, E. P. C. (2023). Origins of transfer establish networks of functional dependencies for plasmid transfer by conjugation. *Nucleic Acids Research*, *51*(7), 3001–3016. https://doi.org/10.1093/nar/gkac1079

Berg, T., Firth, N., Apisiridej, S., Hettiaratchi, A., Leelaporn, A., & Skurray, R. A. (1998). Complete nucleotide sequence of pSK41: evolution of staphylococcal conjugative multiresistance plasmids. *Journal of Bacteriology*, *180*(17), 4350–4359. https://doi.org/10.1128/JB.180.17.4350-4359.1998

Caryl, J. A., & O'Neill, A. J. (2009). Complete nucleotide sequence of pGO1, the prototype conjugative plasmid from the staphylococci. *Plasmid*, *62*(1), 35–38. https://doi.org/10.1016/j.plasmid.2009.03.001

Cazares, A., Figueroa, W., Cazares, D., Lima, L., Turnbull, J. D., McGregor, H., Dicks, J., Alexander, S., Iqbal, Z., & Thomson, N. R. (2025). Pre- and postantibiotic epoch: The historical spread of antimicrobial resistance. *Science*. https://doi.org/10.1126/science.adr1522

Che, Y., Yang, Y., Xu, X., Břinda, K., Polz, M. F., Hanage, W. P., & Zhang, T. (2021). Conjugative plasmids interact with insertion sequences to shape the horizontal transfer of antimicrobial resistance genes. *Proceedings of the National Academy of Sciences of the United States of America*, *118*(6). https://doi.org/10.1073/pnas.2008731118

Choi, W., & Harshey, R. M. (2010). DNA repair by the cryptic endonuclease activity of Mu transposase. *Proceedings of the National Academy of Sciences*, *107*(22), 10014–10019. https://doi.org/10.1073/pnas.0912615107

Deghorain, M., & Van Melderen, L. (2012). The Staphylococci Phages Family: An Overview. *Viruses*, *4*(12), 3316–3335. https://doi.org/10.3390/v4123316

Douarre, P.-E., Mallet, L., Radomski, N., Felten, A., & Mistou, M.-Y. (2020). Analysis of COMPASS, a New Comprehensive Plasmid Database Revealed Prevalence of Multireplicon and Extensive Diversity of IncF Plasmids. *Frontiers in Microbiology*, *11*, 483. https://doi.org/10.3389/fmicb.2020.00483

Fillol-Salom, A., Martínez-Rubio, R., Abdulrahman, R. F., Chen, J., Davies, R., & Penadés, J. R. (2018). Phage-inducible chromosomal islands are ubiquitous within the bacterial universe. *The ISME Journal*, *12*(9), 2114–2128. https://doi.org/10.1038/s41396-018-0156-3

Giordano, C., Barnini, S., Tsioutis, C., Chlebowicz, M. A., Scoulica, E. V., Gikas, A., Rossen, J. W., Friedrich, A. W., & Bathoorn, E. (2018). Expansion of KPC-producing Klebsiella pneumoniae with various mgrB mutations giving rise to colistin resistance: the role of IS L3 on plasmids. *International Journal of Antimicrobial Agents*, *51*(2), 260–265. https://doi.org/10.1016/j.ijantimicag.2017.10.011

Gómez-Sanz, E., Zarazaga, M., Kadlec, K., Schwarz, S., & Torres, C. (2013). Chromosomal integration of the novel plasmid pUR3912 from methicillin-susceptible Staphylococcus aureus ST398 of human origin. *Clinical Microbiology and Infection*, *19*(11), E519–E522. https://doi.org/10.1111/1469-0691.12279

Goswami, C., Fox, S., Holden, M. T. G., Connor, M., Leanord, A., & Evans, T. J. (2020). Origin, maintenance and spread of antibiotic resistance genes within plasmids and chromosomes of bloodstream isolates of Escherichia coli. *Microbial Genomics*, *6*(4). https://doi.org/10.1099/mgen.0.000353

Harmer, C. J., Moran, R. A., & Hall, R. M. (2014). Movement of IS *26* -Associated Antibiotic Resistance Genes Occurs via a Translocatable Unit That Includes a Single IS *26* and Preferentially Inserts Adjacent to Another IS *26*. *MBio*, *5*(5). https://doi.org/10.1128/mBio.01801-14

He, S., Hickman, A. B., Varani, A. M., Siguier, P., Chandler, M., Dekker, J. P., & Dyda, F. (2015a). Insertion Sequence IS 26 Reorganizes Plasmids in Clinically Isolated Multidrug-Resistant Bacteria by Replicative Transposition. *MBio*, *6*(3), e00762. https://doi.org/10.1128/mBio.00762-15

He, S., Hickman, A. B., Varani, A. M., Siguier, P., Chandler, M., Dekker, J. P., & Dyda, F. (2015b). Insertion Sequence IS26 Reorganizes Plasmids in Clinically Isolated Multidrug-Resistant Bacteria by Replicative Transposition. *MBio*, *6*(3), e00762. https://doi.org/10.1128/mBio.00762-15

Humphrey, S., Millán, Á. S., Toll-riera, M., Connolly, J., Flor-duro, A., Chen, J., Ubeda, C., Maclean, R. C., & Penadés, J. R. (2021). Staphylococcal phages and pathogenicity islands drive plasmid evolution. *Nature Communications*. https://doi.org/10.1038/s41467-021-26101-5

Kouprina, N., & Larionov, V. (2008). Selective isolation of genomic loci from complex genomes by transformation-associated recombination cloning in the yeast *Saccharomyces cerevisiae*. *Nature Protocols*, *3*(3), 371–377. https://doi.org/10.1038/nprot.2008.5

Lee, N. C. O., Larionov, V., & Kouprina, N. (2015). Highly efficient CRISPR/Cas9-mediated TAR cloning of genes and chromosomal loci from complex genomes in yeast. *Nucleic Acids Research*, *43*(8), e55. https://doi.org/10.1093/nar/gkv112

Leelaporn, A., Firth, N., Paulsen, I. T., & Skurray, R. A. (1996). IS257-mediated cointegration in the evolution of a family of staphylococcal trimethoprim resistance plasmids. *Journal of Bacteriology*, *178*(20), 6070–6073. https://doi.org/10.1128/jb.178.20.6070-6073.1996

Liu, H., Tu, Y., He, J., Xu, Q., Zhang, X., Mu, X., Chen, M., Zhou, H., & Li, X. (2024). Emergence and plasmid cointegration-based evolution of NDM-1-producing ST107 Citrobacter freundii high-risk resistant clone in China. *International Journal of Antimicrobial Agents*, *63*(2), 107069. https://doi.org/10.1016/j.ijantimicag.2023.107069

Liu, Z., Tang, Y., He, M., & Xu, C. (2025). Molecular drivers of fusion plasmid: mechanistic insights and evolutionary implications. *Journal of Antimicrobial Chemotherapy*, *80*(11), 2902–2911. https://doi.org/10.1093/jac/dkaf309

Morton, T. M., Johnston, J. L., Patterson, J., & Archer, G. L. (1995). Characterization of a conjugative staphylococcal mupirocin resistance plasmid. *Antimicrobial Agents and Chemotherapy*, *39*(6), 1272–1280. https://doi.org/10.1128/AAC.39.6.1272

Novick, R. P. (1987). Plasmid incompatibility. *Microbiological Reviews*, *51*(4), 381–395. https://doi.org/10.1128/mr.51.4.381-395.1987

Novick, R. P., Edelman, I., & Lofdahl, S. (1986). Small Staphylococcus aureus plasmids are transduced as linear multimers that are formed and resolved by replicative processes. *Journal of Molecular Biology*, *192*(2), 209–220. https://doi.org/10.1016/0022-2836(86)90360-8

Osborn, A. M., da Silva Tatley, F. M., Steyn, L. M., Pickup, R. W., & Saunders, J. R. (2000). Mosaic plasmids and mosaic replicons: evolutionary lessons from the analysis of genetic diversity in IncFII-related replicons The EMBL accession numbers for the sequences reported in this paper are AJ009980 (pGSH500 alpha replicon) and AJ009981 (pLV1402 alpha replicon). *Microbiology*, *146*(9), 2267–2275. https://doi.org/10.1099/00221287-146-9-2267

Partridge, S. R., Kwong, S. M., Firth, N., & Jensen, S. O. (2018). Mobile Genetic Elements Associated with Antimicrobial Resistance. *Clinical Microbiology Reviews*, *31*(4). https://doi.org/10.1128/CMR.00088-17

Pfeifer, E., & Rocha, E. P. C. (2024). Phage-plasmids promote recombination and emergence of phages and plasmids. *Nature Communications*, *15*(1), 1545. https://doi.org/10.1038/s41467-024-45757-3

Rozwandowicz, M., Brouwer, M. S. M., Fischer, J., Wagenaar, J. A., Gonzalez-Zorn, B., Guerra, B., Mevius, D. J., & Hordijk, J. (2018). Plasmids carrying antimicrobial resistance genes in Enterobacteriaceae. *Journal of Antimicrobial Chemotherapy*, *73*(5), 1121–1137. https://doi.org/10.1093/jac/dkx488

Ruiz, E., Talenton, V., Dubrana, M.-P., Guesdon, G., Lluch-Senar, M., Salin, F., Sirand-Pugnet, P., Arfi, Y., & Lartigue, C. (2019). CReasPy-Cloning: A Method for Simultaneous Cloning and Engineering of Megabase-Sized Genomes in Yeast Using the CRISPR-Cas9 System. *ACS Synthetic Biology*, *8*(11), 2547–2557. https://doi.org/10.1021/acssynbio.9b00224

Sastre-Dominguez, J., DelaFuente, J., Toribio-Celestino, L., Herencias, C., Herrador-Gómez, P., Costas, C., Hernández-García, M., Cantón, R., Rodríguez-Beltrán, J., Santos-Lopez, A., & San Millan, A. (2024). Plasmid-encoded insertion sequences promote rapid adaptation in clinical enterobacteria. *Nature Ecology & Evolution*. https://doi.org/10.1038/s41559-024-02523-4

Savoldi, A., Carrara, E., Gladstone, B. P., Azzini, A. M., Göpel, S., & Tacconelli, E. (2019). Gross national income and antibiotic resistance in invasive isolates: analysis of the top-ranked antibiotic-resistant bacteria on the 2017 WHO priority list. *Journal of Antimicrobial Chemotherapy*, *74*(12), 3619–3625. https://doi.org/10.1093/jac/dkz381

Smillie, C., Garcillán-Barcia, M. P., Francia, M. V., Rocha, E. P. C., & de la Cruz, F. (2010). Mobility of Plasmids. *Microbiology and Molecular Biology Reviews*, *74*(3), 434–452. https://doi.org/10.1128/MMBR.00020-10

Snaith, A. E., Dunn, S. J., Moran, R. A., Newton, P. N., Dance, D. A. B., Davong, V., Kuenzli, E., Kantele, A., Corander, J., & McNally, A. (2023). The highly diverse plasmid population found in Escherichia coli colonizing travellers to Laos and its role in antimicrobial resistance gene carriage. *Microbial Genomics*, *9*(5). https://doi.org/10.1099/mgen.0.001000

Varani, A., He, S., Siguier, P., Ross, K., & Chandler, M. (2021). The IS6 family, a clinically important group of insertion sequences including IS26. *Mobile DNA*, *12*(1), 11. https://doi.org/10.1186/s13100-021-00239-x

Vos, M., & Didelot, X. (2009). A comparison of homologous recombination rates in bacteria and archaea. *The ISME Journal*, *3*(2), 199–208. https://doi.org/10.1038/ismej.2008.93

Wang, X., Tang, B., Liu, G., Wang, M., Sun, J., Tan, R., Pan, T., Qu, J., Liu, J., Ou, H.-Y., & Qu, H. (2022). Transmission of Nonconjugative Virulence or Resistance Plasmids Mediated by a Self-Transferable IncN3 Plasmid from Carbapenem-Resistant Klebsiella pneumoniae. *Microbiology Spectrum*, *10*(4). https://doi.org/10.1128/spectrum.01364-22

World-Health-Organization. (2022). *Emerging trends and technologies: a horizon scan for global public health*. https://iris.who.int/server/api/core/bitstreams/8e39c847-cd46-413d-ae11-8098ca841011/content

Yui Eto, K., Firth, N., Davis, A. M., Kwong, S. M., Krysiak, M., Lee, Y. T., O'Brien, F. G., Grubb, W. B., Coombs, G. W., Bond, C. S., & Ramsay, J. P. (2019). Evolution of a 72-Kilobase Cointegrant, Conjugative Multiresistance Plasmid in Community-Associated Methicillin-Resistant Staphylococcus aureus Isolates from the Early 1990s. *Antimicrobial Agents and Chemotherapy*, *63*(11). https://doi.org/10.1128/AAC.01560-19

Figure 09/01/26

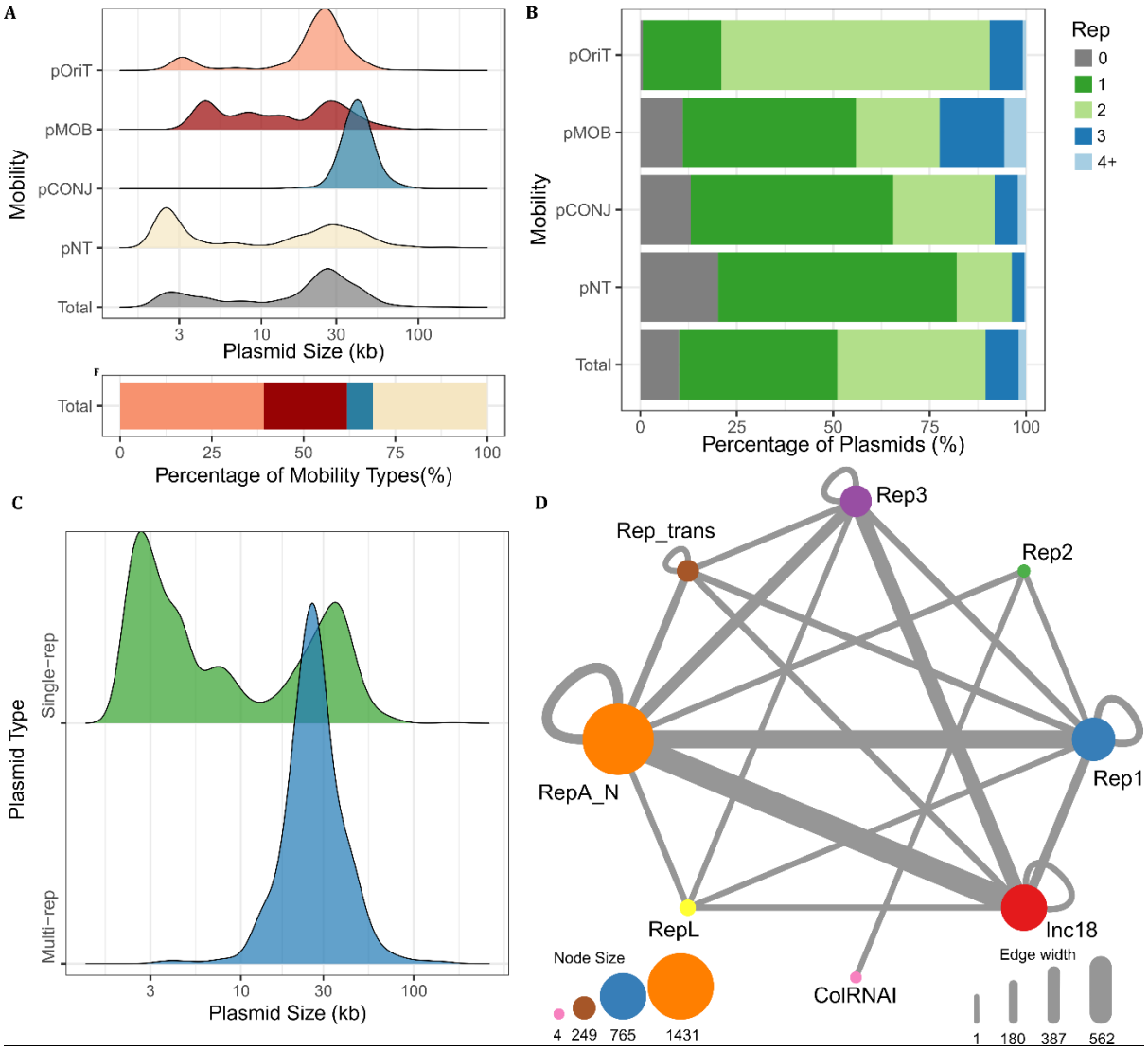

Figure 1: Analysis of mobility and replicon types of 2,564 complete *Staphylococcus* plasmids. pConj: Conjugative, pMob: mobilizable, pOriT: carrying oriT, pNT: Non-trnasmissible. **A-** Top: Density plot of plasmid size (log10 transformed) by mobility type (pOriT, pMOB, pCONJ and pNT). Bottom: Proportion of plasmids assigned to four mobility types (same color palette in top). **B-**Proportion of plasmids encoding 1-4 replicon(s) by mobility types, plasmids with more than four replicons are merged into "4+" group, plasmids encoding replicon not identifiable are in group "0". **C-** Size comparision between single- and multi-replicon plasmids. **D-** Replicon co-occurrence network for multi-replicon plasmids. Nodes represent plasmid replicon families; node size is proportional to the number of replicons. Edges and self-loops indicate co-occurrence of two replicons from different and the same families on the same plasmid; edge thickness reflects the number of co-occurrence instances. Rolling-circle replicon: Rep1, Rep2, RepL, Rep_trans; theta replication: RepA_N, Inc18, Rep3, ColRNAI.

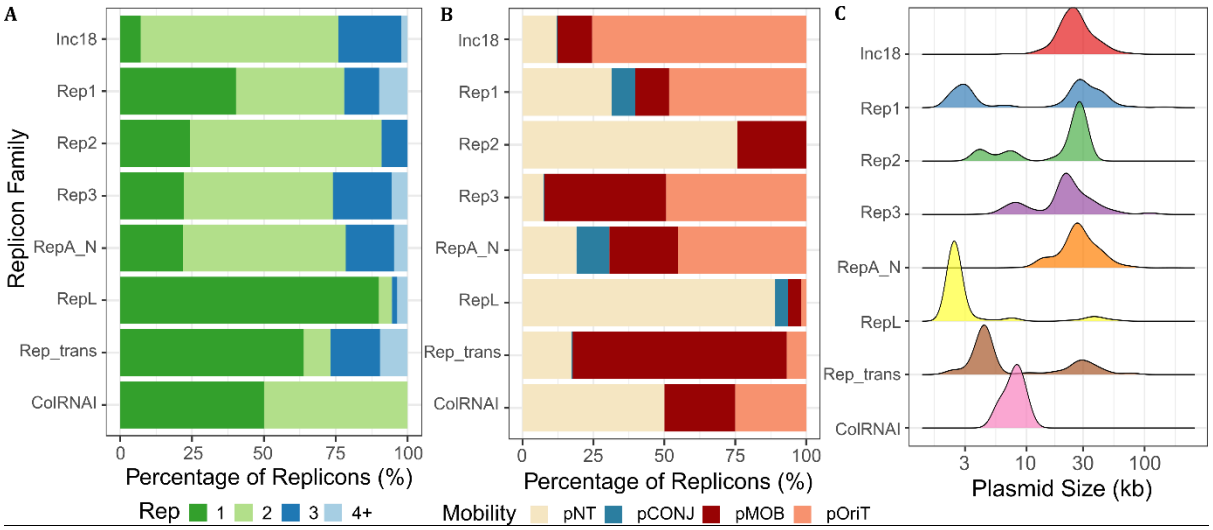

Figure S1: Distribution of plasmid replicon families in *Staphylococcus*. A- Proportion of plasmid encoding 1-4+ replicon(s) within each replicon family, plasmids encoding more than four replicons are merged into "4+" group. **B-** Distribution of plasmid mobility types within replicon family. **C-** Comparison of plasmid size (log10 transformed) across replicon family.

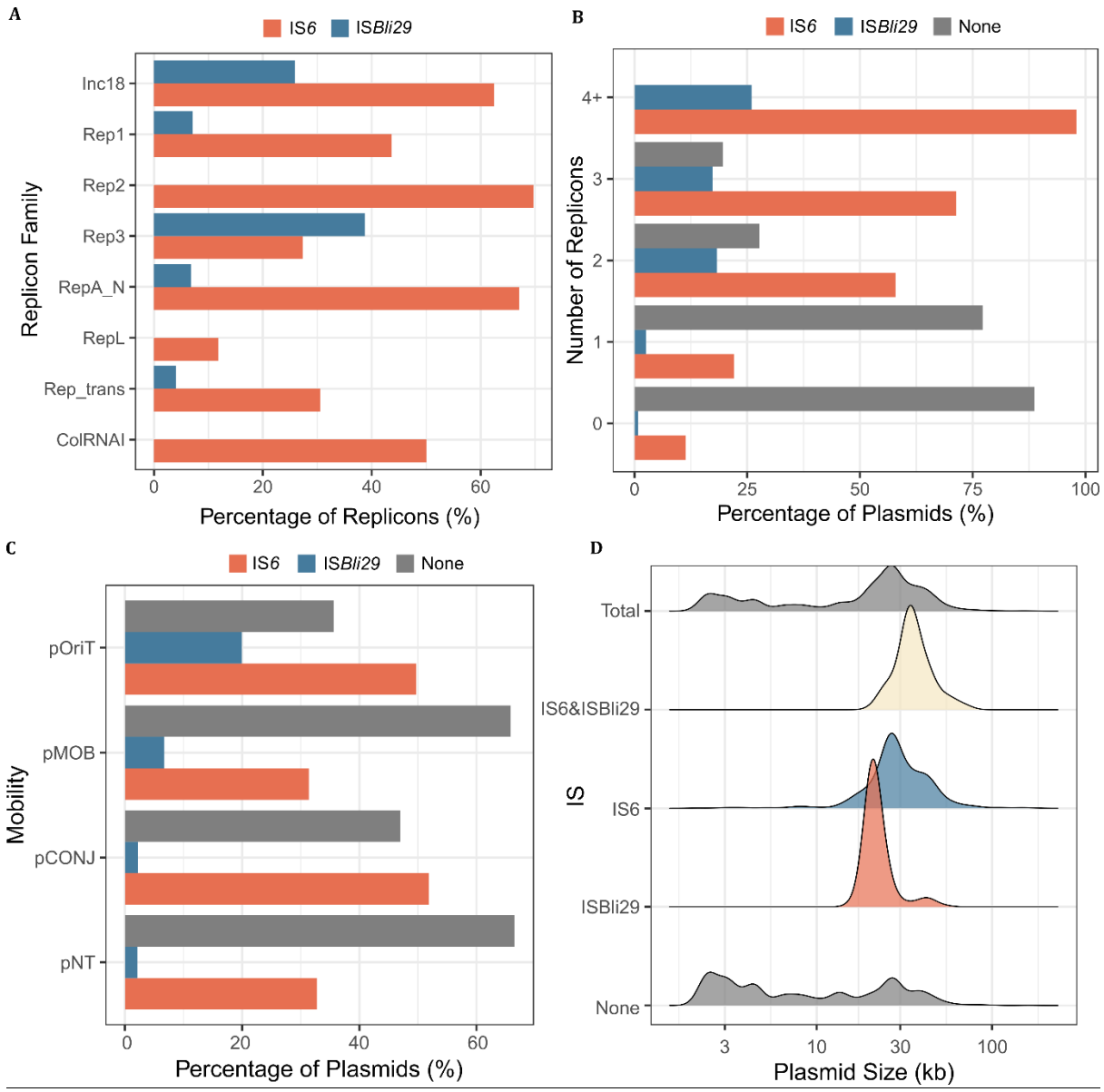

Figure S2: Distribution of Insertion Sequence (IS) IS*6* and IS*Bli29* in *Staphylococcus* plasmids. A- Frequency of IS*6* and IS*Bli29* in plasmids grouped by replicon family. **B-** Proportion of IS*6* and IS*Bli29* encoding plasmids with 1-4+ replicon(s), plasmids with more than four replicons are merged into "4+" group, plasmid encoding replicon not identifiable are in group "0". **C-** Proportion of IS*6* and IS*Bli29* encoding plasmids by mobility types. **D-** Comparision of plasmid size by encoding IS*6*, IS*Bli29*, both, and neither. (Note: 97.6% of the IS*6* here is cross valid by ISfinder as IS*6* family clade f, i.e. IS*257*; IS*Bli29* here is the ORF4 which encodes a transposase with a Mu transposase C-terminal domain, pfam accession PF09299).

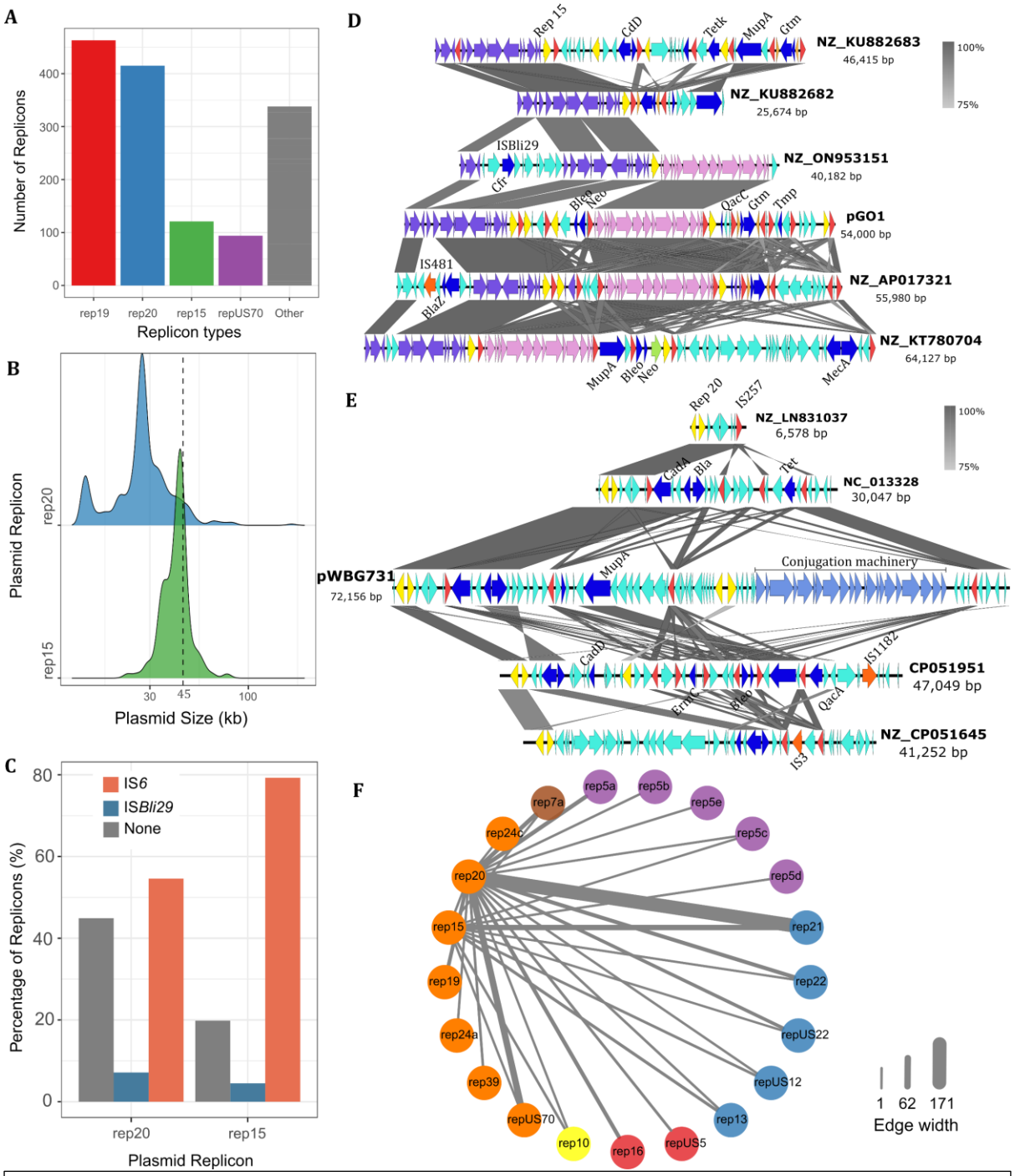

Figure 2: Rep15 and Rep20 plasmids. A- Replicon types in RepA_N family. (Rare replicon types are grouped into 'Other') **B-** Size comparision between plasmids encoding rep15 and rep20 replicon. **C-** Proportion of IS*6* and IS*Bli29* in plasmids encoding rep15 and rep20. **D-** Plasmid alignment of selected examples for Rep 15 plasmid family. **E-** Plasmid alignment of selected examples for Rep 20 plasmid family. **F-** Replicon co-occurrence network for plasmids encoding rep15 and rep20. Nodes represent plasmid replicon types, colored by replicon familes (the same color palette in **Fig. 1**, Theta replicon: RepA_N in orange, Inc18 in red, Rep3 in purple; Rolling-circle replicon: Rep1 in blue, Rep2 in green, RepL in yellow, Rep_trans in brown). Edges indicate co-occurrence of two replicon type on the same plasmid; edge thickness reflects the number of co-occurrence instances.

Table1: Binomial generalized linear model for multi- / single- replicon plasmid

Predictor	Estimate	95% CI	z-value	P-value
Intercept	-20.16	[-22.39,-18.04]	-18.19	<0.001
Log10(Size)	4.27	[3.79,4.79]	16.68	<0.001
IS_presence	1.06	[0.78,1.35]	7.24	<0.001
Mobility(pOriT)	2.98	[2.65,3.32]	17.35	<0.001
Mobility(pMOB)	2.19	[1.73,2.48]	11.00	<0.001
Mobility(pCONJ)	-0.71	[-1.13,-0.28]	-3.28	<0.01

AIC: 1647.4

Table 1: Rep15 and Rep20 plasmids. Plasmid encoding multiple- / single-replicon was analyzed using a binomial glm with a logit link. Plasmid size shows siginificant effect, IS_presence (presence of either IS*6* or IS*Bli29*) also had an independent significant effect. Compared to plasmid lacking mobility (pNT), pOriT and pMOB show significant effect, pCONJ shows moderate effect.

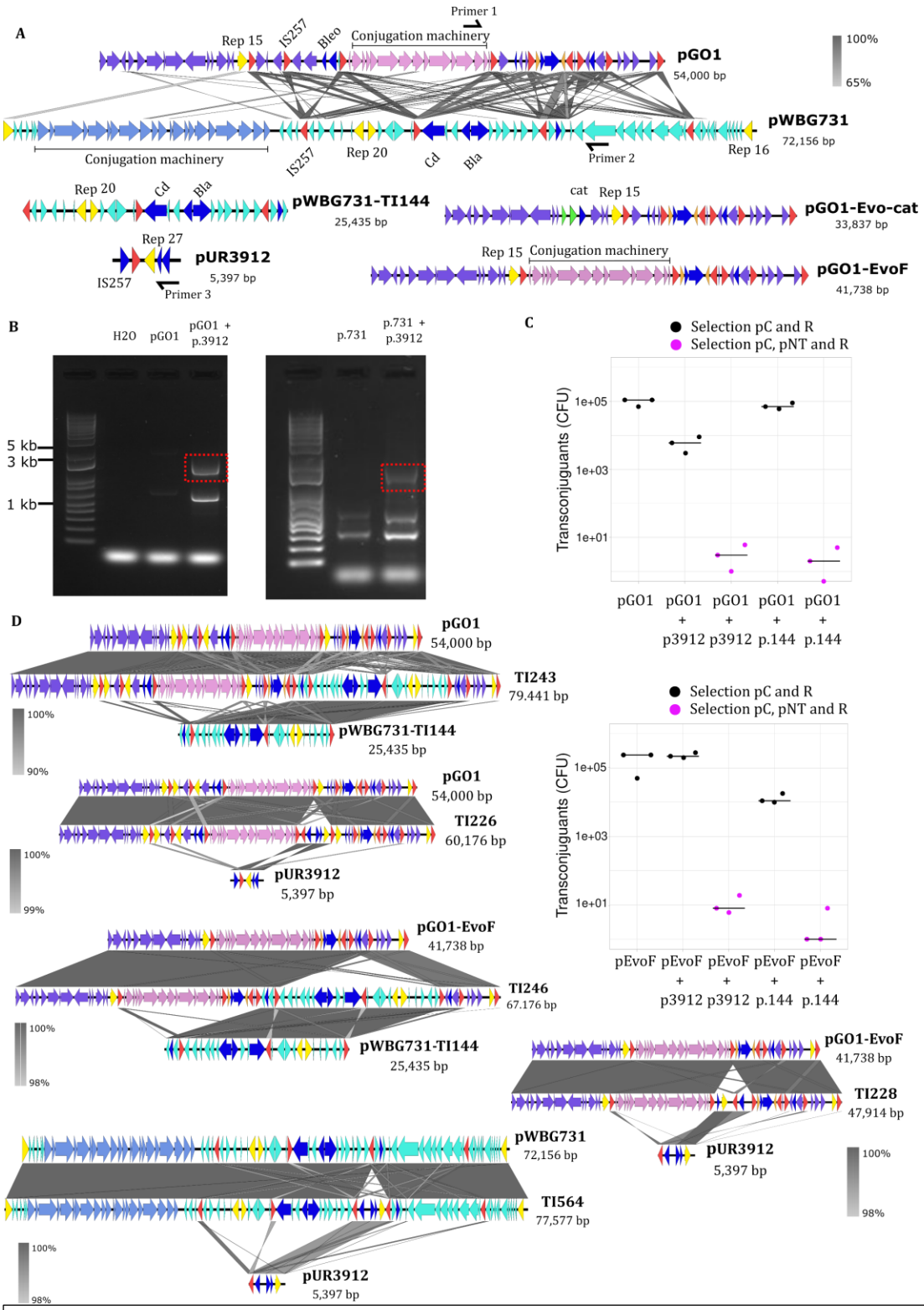

Figure S3 : Plasmid fusion assays. A- Plasmids map used in this study. Gtm: gentamycin resistance, Cd: Cadmium resistance, Tmp: Trimethoprim resistance, Ery: Erythromycin resistance. Primer designed for the detection of fusion events on pGO1 and pWBG731 plasmids with pUR3912 are represented. **B-** Detection of fusion events within pGO1 and pUR3912 IS257 and pWBG731 and pUR3912. **C-** Experience of plasmid fusion with the conjugative pGO1 AND pGOI1-EvoF plasmid. p.3912 (pUR3912), p.144 (pWBG731-TI144), p.Evo (pGO1-Evocat). Conjugation controls have been used by selecting only for the conjugative plasmid and the recipient strain (Black dots). **D-** Other examples of plasmid fusion events sequenced by Long-Read sequencing.

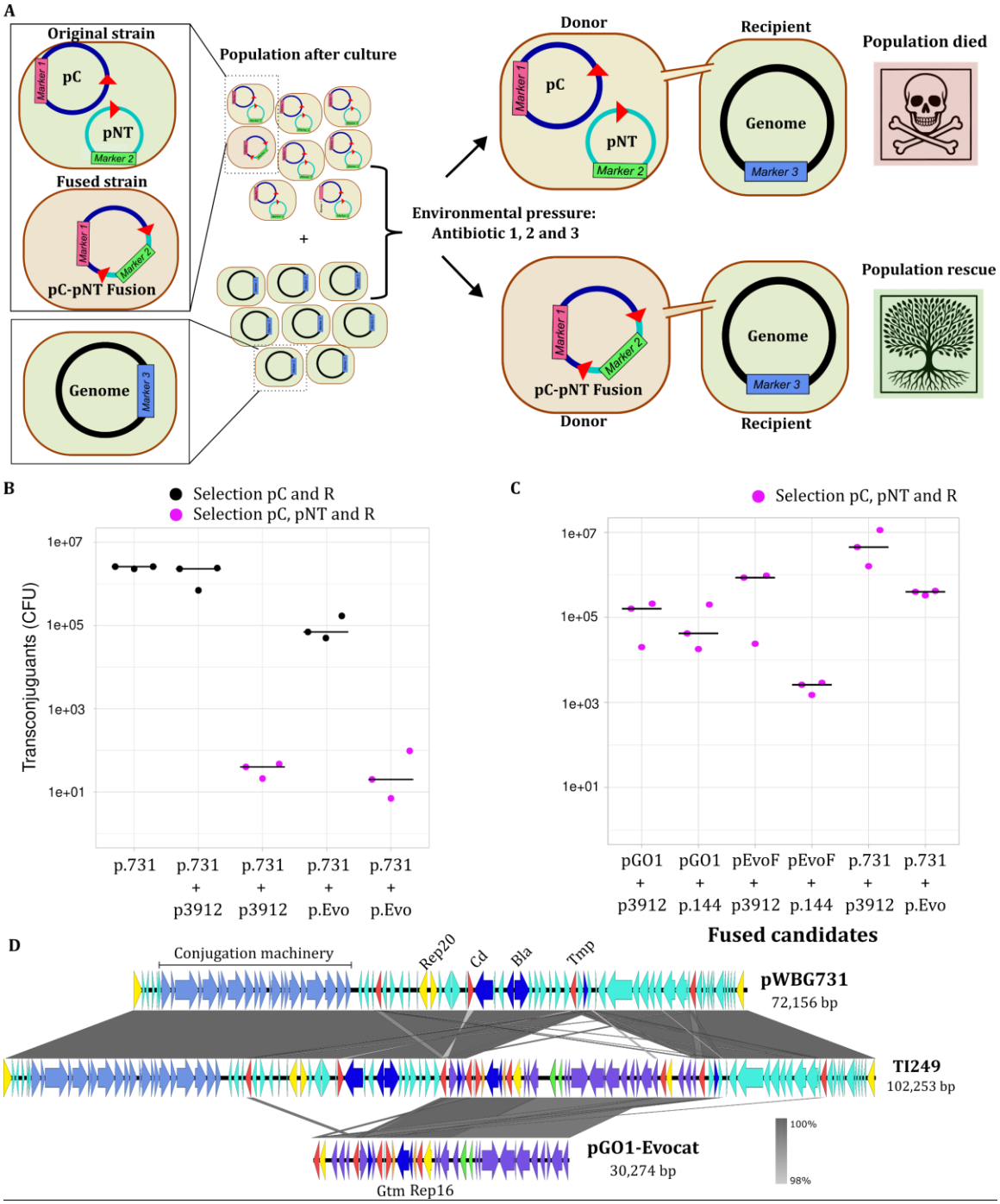

Figure 3: Plasmid fusion is selected during strong antibiotic pressure and rescue *S. aureus* population. A- Graphical representation where plasmid fusion event would rescue the population during environmental pressure. pC (Conjugative plasmid), pNT (Non-transmissible plasmid). Red Triangle represent any sequence that would bring homology for fusion between two plasmid. In the case of pGO1, pWBG731, pUR3912, this is *IS257* gene. **B-** Experience of plasmid fusion with the conjugative pWBG731 plasmid. p.3912 (pUR3912), p.144 (pWBG731-TI144), p.Evo (pGO1-Evocat). Conjugation controls have been used by selecting only for the conjugative plasmid and the recipient strain (Black dots). **C-** Experience of conjugation made from colony obtained after fusion experiment (in B). **D-** Examples of plasmid fusion events sequenced by Long-Read sequencing. Gtm : gentamycin resistance, Cd: Cadmium resistance, Tmp: Trimethoprim resistance.

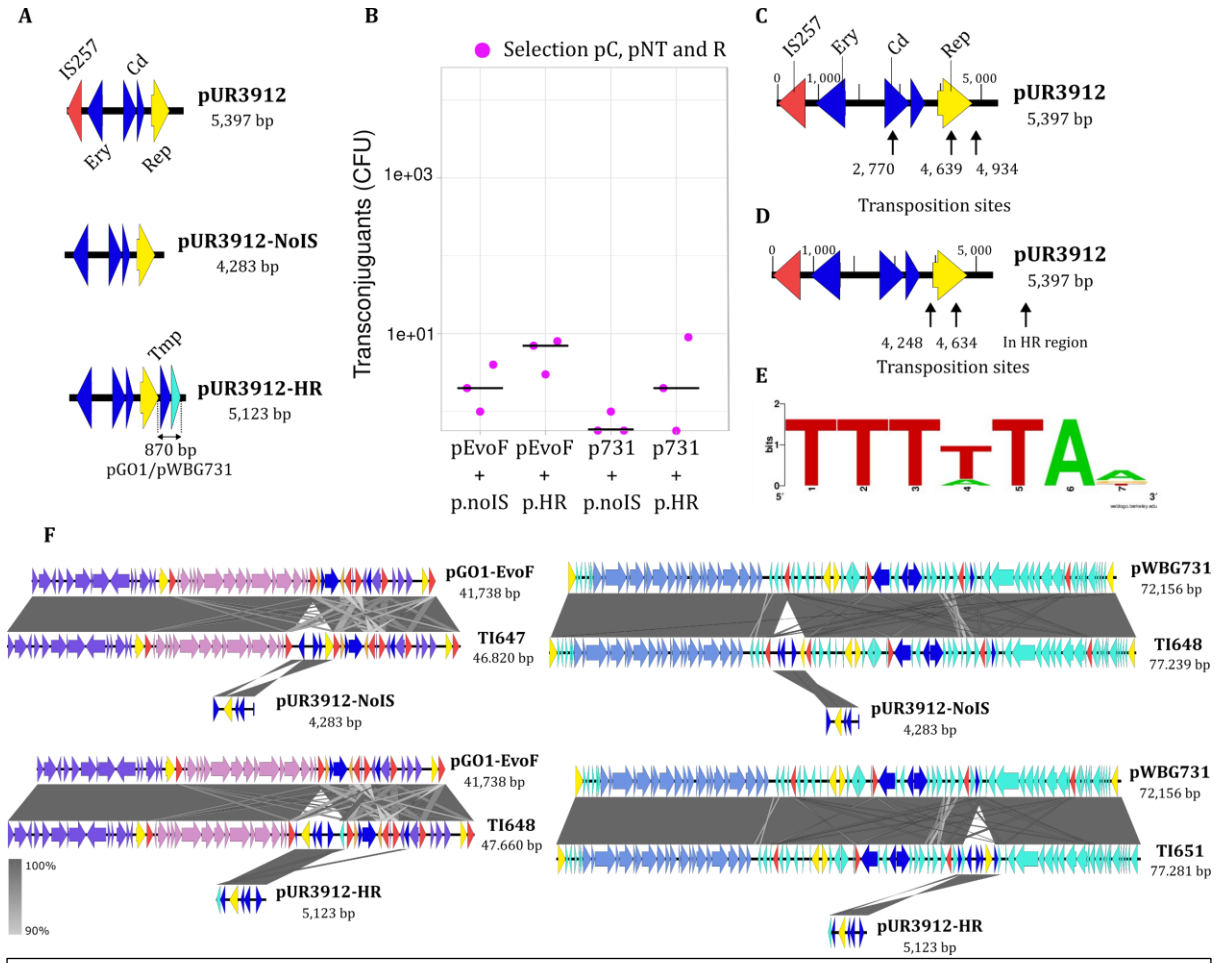

Figure S4 : Plasmid fusion is issued from both HR or Tp events. A- Derivative plasmid from pUR3912 after *IS257* gene removing or replaced by another gene find in both pGO1 and pWBG731. **B-** Experience of plasmid fusion with pUR3912 derivates to test homologous recombination (HR) and transposition (Tp) mechanisms. **C-** Sites of transposition in pC-pUR3912 fusion plasmids. **D- -** Sites of transposition in pC-pUR3912 derivates fusion plasmids. **E-** Consensus motif for transposition site. **F-** Examples of plasmid fusion events sequenced by Long-Read sequencing.

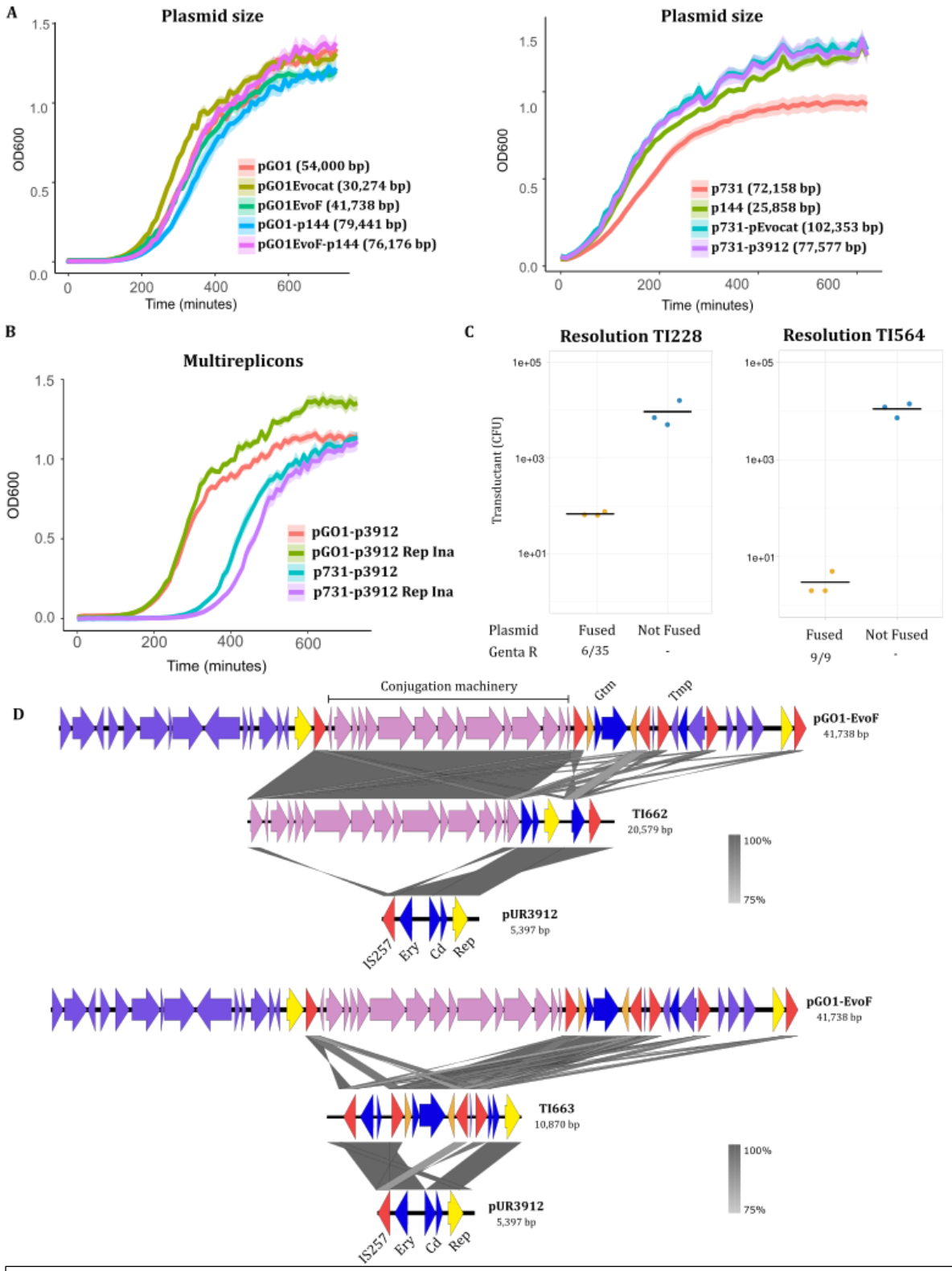

Figure 4 : Plasmids size limitation is not linked to fitness or resolution mechanism after plasmid fusion. A- Growth curve of plasmid issued from pGO1 family, his fused version and the smaller versions and Growth curve of plasmid issued from pWBG731 family, his fused version and the smaller versions. **B**- Growth curve of plasmid having multi-replicons that are functional or not obtained after plasmid fusions. **C**- Plasmid resolution efficiency detected after phage transduction of and selection only of the small plasmid pUR3912 if resolved after fusion. Number of colonies still resistant to the big fused plasmid is represented. **D-** Example of sequenced clones obtained after the plasmid resolution assay.

A

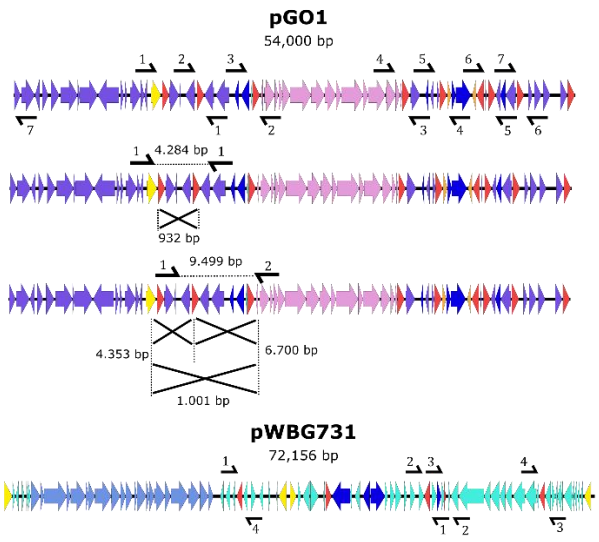

C

	Primers	WT size	Rec.size	Amplification	Sanger val.
pGO1	1	4284	932	Y	nd
	2	6345	999	Y	nd
	3	15377	974	Y	nd
	4	4948	1384	Y	Y
	5	5682	988	Y	Y
	6	4081	1346	Y	Y
	7	5925	1034	Y	nd
	1F/2R	9699	1001	Y	nd
	1F/4R	28075	1410	Y	nd
	1F/7R	40042	1057	N	nd
pWBG731	1	23822	924	Y	Y
	2	3195	626	Y	Y
	3	12617	1079	Y	Y
	4	36347	1148	Y	nd
	1F/2R	26108	667	Y	nd
	2F/4R	50357	1097	Y	nd
	3F/4R	47928	1211	Y	nd

B

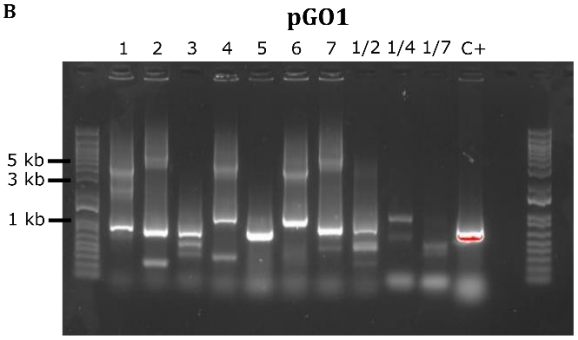

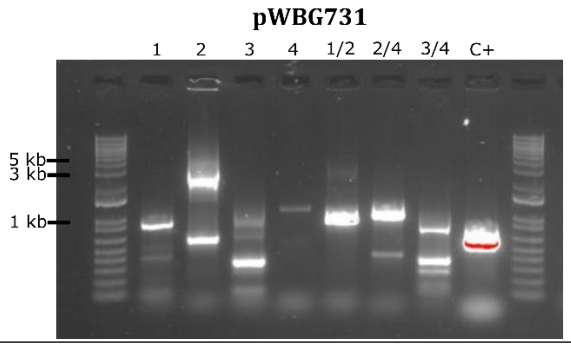

Figure S5 : Detection of deletion events in bacterial cell population. A- Design of the primers for detection of deletion in pGO1 and pWBG731 between differents copies of IS257. **B**- Detection by PCR of Recombination scars. **C**- Recapitulative table of deletion detection results.

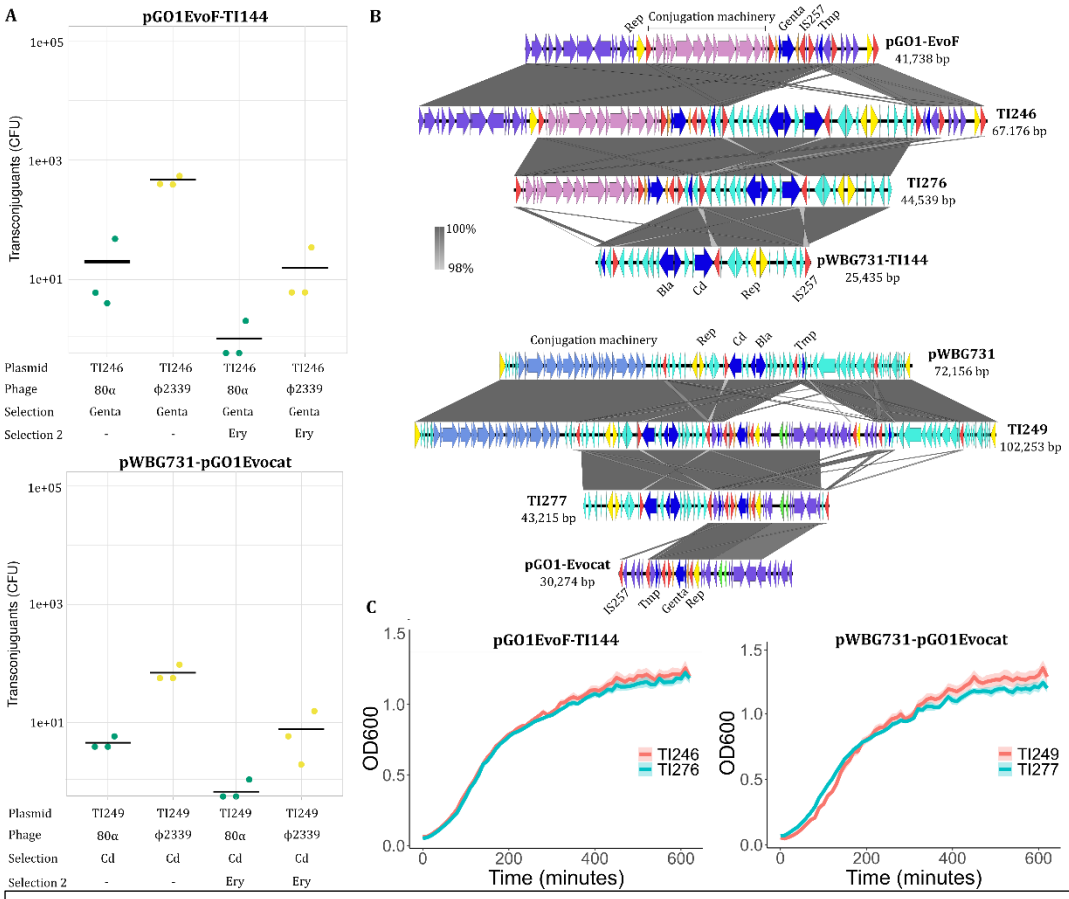

Figure 5 : Phage select for diverse intermediate size plasmid derivate. **A-** transduction of TI246, the fused version pGO1EvoF/pWBG731-TI144 and TI249, the fused version pWBG731/pGO1Evocat. **B-** Sequence alignment of derivates obtain after transduction. **C-** Growth curve of plasmid fused version vs transduce version.

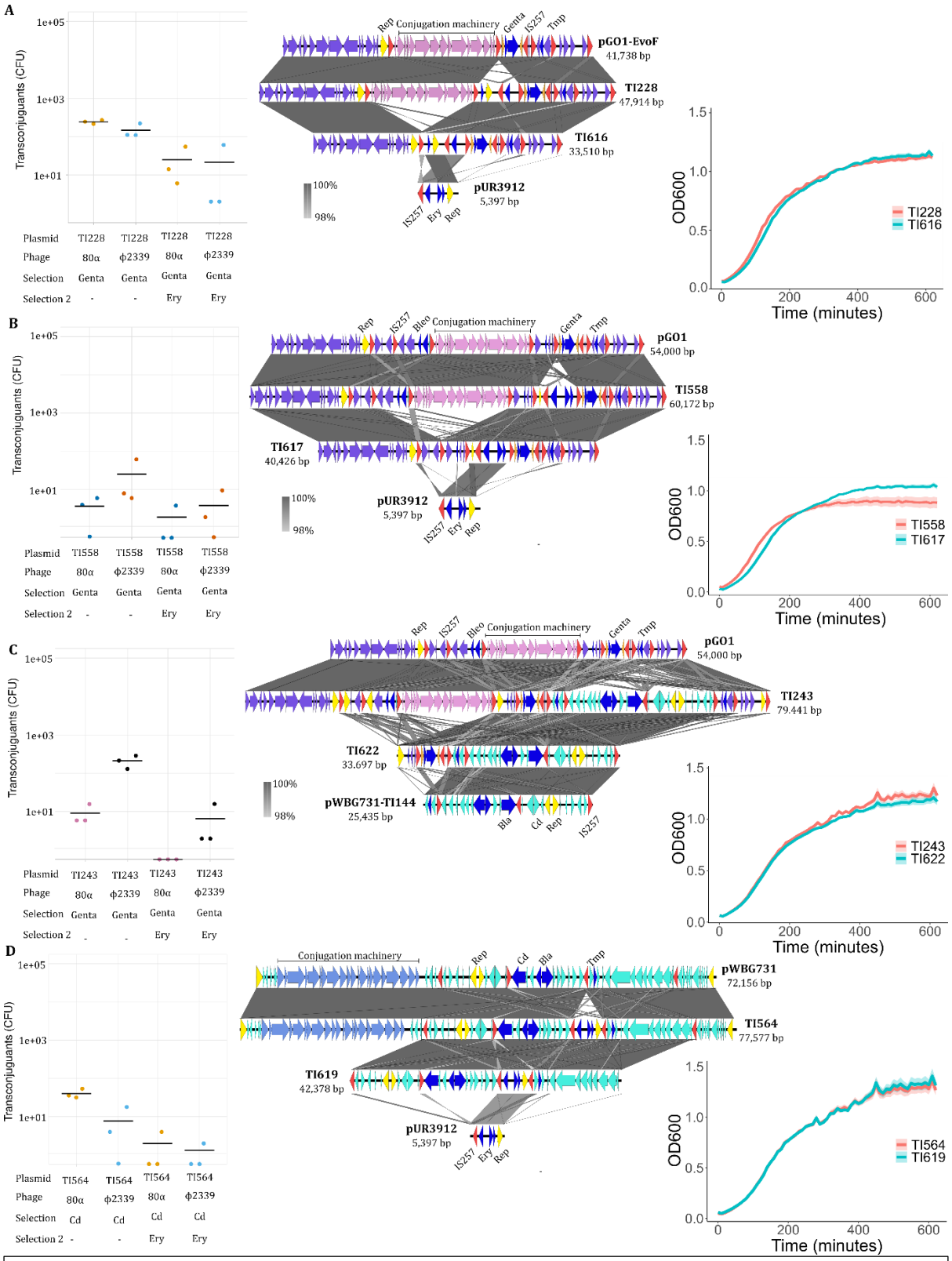

Figure S6 : Phage select for diverse intermediate size plasmid derivate. A- Result obtained for TI228, the fused version pGO1EvoF/pUR3912, after Transduction, the sequence alignment of derivates obtain after transduction and the growth curve of plasmid fused version vs transduce version. **B**- Same for TI558 the fused version pGO1/pUR3912. **C**- Same for TI243 the fused version pGO1/pWBG731-TI144. **D**- Same for TI564 the fused version pWBG731/pUR3912.